

Smart grids: from traditional to modernized resilient systems

Víctor Escala García
Josep Fanals Batllori
Pol Heredia Julbe
Roger Izquierdo Toro
Palina Nicolas

Smart Grids

January 13, 2021

Smart grids: from
traditional to
modernized
resilient systems

Group 2

Introduction

Phase 1

Results

Problems identification

Context

Aim of the project

Models

General scheme

MPPT

Machine-side converter

Grid-side converter

Supercapacitor control

Sizing

Calculations

Configuration

Results

Indicators

Example

Conclusions

2 / 23

1. Introduction

2. Phase 1

2.1 Results

2.2 Problems identification

2.3 Context

2.4 Aim of the project

3. Models

3.1 General scheme

3.2 MPPT

3.3 Machine-side converter

3.4 Grid-side converter

3.5 Supercapacitor control

4. Sizing

4.1 Calculations

4.2 Configuration

5. Results

5.1 Indicators

5.2 Example

6. Conclusions

7. Bibliography

- ▶ Smart grids are becoming a necessity in order to integrate renewables, accommodate new actors, improve the observability and efficiency.
- ▶ The transition from conventional systems towards smart grids is challenging:
 - ▶ Incorporate distributed sources of energy.
 - ▶ Integrate storage systems.
 - ▶ Rely less on large traditional centralized power plants.

Thus, we have divided the progressive adaptations:

Chapter	Activities
Phase 1	Initial solution of the system
Phase 2	Addition of lines
Phase 3	Integration of wind and solar
Phase 4	Rehabilitated power plant and storage
SGAM	HLUC related to contingencies

Table 1: Phases of the project to move towards smart grids

Smart grids: from traditional to modernized resilient systems

Group 2

Introduction

Phase 1

Results

Problems identification

Context

Aim of the project

Models

General scheme

MPPT

Machine-side converter

Grid-side converter

Supercapacitor control

Sizing

Calculations

Configuration

Results

Indicators

Example

Conclusions

4 / 23

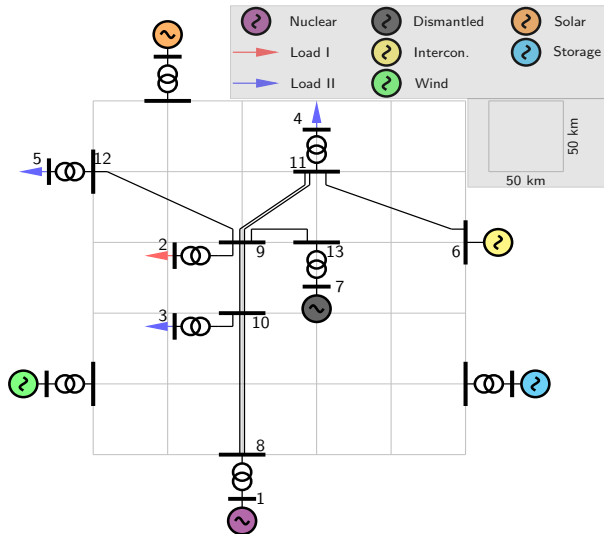


Figure 1: Overview of the network

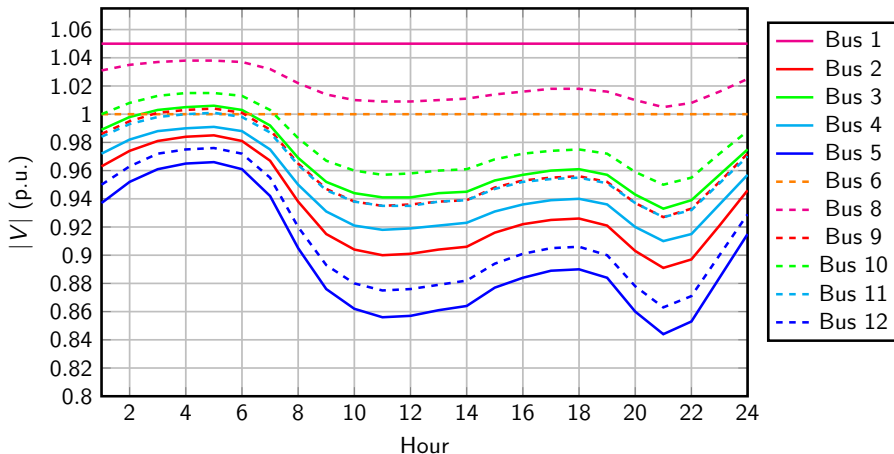


Figure 2: Voltage profile during 24 hours for the initial grid. The low-voltage buses are plotted in solid lines; the high-voltage ones are in dashed lines.

Smart grids: from traditional to modernized resilient systems

Group 2

Introduction

Phase 1

Results

Problems identification

Context

Aim of the project

Models

General scheme

MPPT

Machine-side converter

Grid-side converter

Supercapacitor control

Sizing

Calculations

Configuration

Results

Indicators

Example

Conclusions

6 / 23

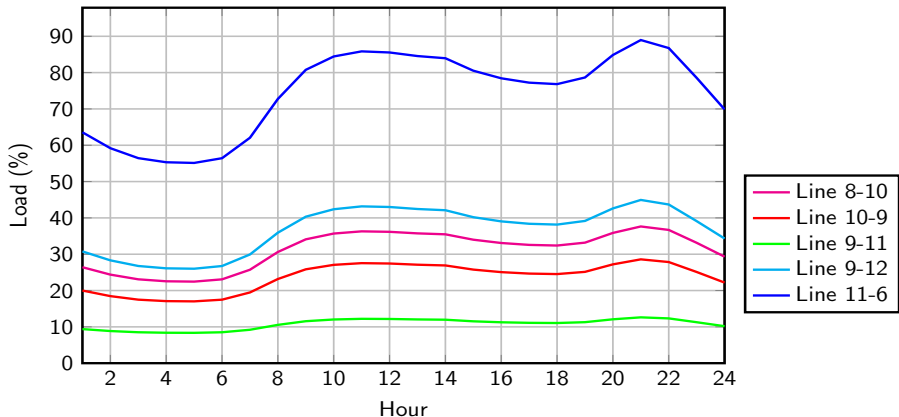


Figure 3: Representation of the percentual loading of the lines during 24 hours

The main observed issues are:

- ▶ Some load buses are below 0.9 p.u. during peak hours.
- ▶ While no lines surpass 100% of load, the interconnection line is close to 90%.
- ▶ In addition, the $N - 1$ criteria is not met:

Element	Disconnection time (h)	Consequences
Line 8-10	12.50	No load served - divergence
Line 9-10	6.25	No load served - divergence
Line 9-11	8.85	Loads at buses 2, 3 and 5 unserved
Line 9-12	13.98	Load at bus 5 unserved
Line 11-6	13.98	No load served
Trafo 1-8	1.20	No load served - divergence
Trafo 2-9	1.20	Load at bus 2 unserved
Trafo 3-10	1.20	Load at bus 3 unserved
Trafo 4-11	1.20	Load at bus 4 unserved
Trafo 5-12	1.20	Load at bus 5 unserved

Table 2: Disconnection time and consequences of losing each element

- ▶ Wind speeds exhibit unpredictable fluctuations.
- ▶ These variations in wind speed cause drastic changes in power:

$$P_{wt} = \frac{1}{2} \rho A C_p v_w^3. \quad (1)$$

Store the peaks of power and retrieve the energy once the wind speed diminishes.

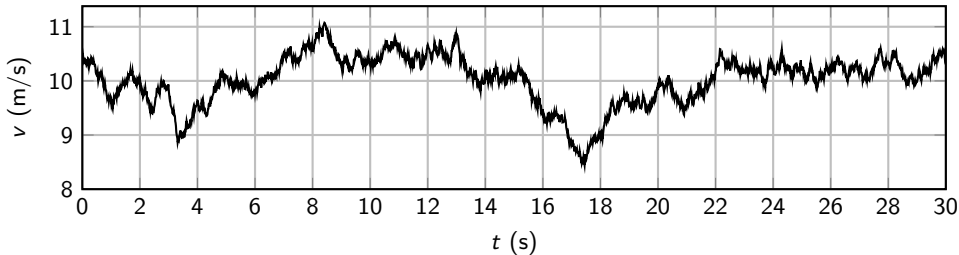


Figure 4: Example of wind speed profile

Smart grids: from
traditional to
modernized
resilient systems

Group 2

Introduction

Phase 1

Results

Problems identification

Context

Aim of the project

Models

General scheme

MPPT

Machine-side converter

Grid-side converter

Supercapacitor control

Sizing

Calculations

Configuration

Results

Indicators

Example

Conclusions

9/23

Goals:

- ▶ Minimize the fluctuations in the power exchanged with the grid.
- ▶ Ensure the supercapacitor operates inside the allowed limits.
- ▶ Quantify the results and compare them with other techniques.

Steps:

1. Model the back-to-back converter configuration of a wind turbine.
2. Size the energy storage unit (supercapacitor).
3. Model the control of a buck converter to integrate the supercapacitor.
4. Test the full model in Matlab/Simulink for a realistic scenario.

Smart grids: from traditional to modernized resilient systems

Group 2

Introduction

Phase 1

Results

Problems identification

Context

Aim of the project

Models

General scheme

MPPT

Machine-side converter

Grid-side converter

Supercapacitor control

Sizing

Calculations

Configuration

Results

Indicators

Example

Conclusions

10 / 23

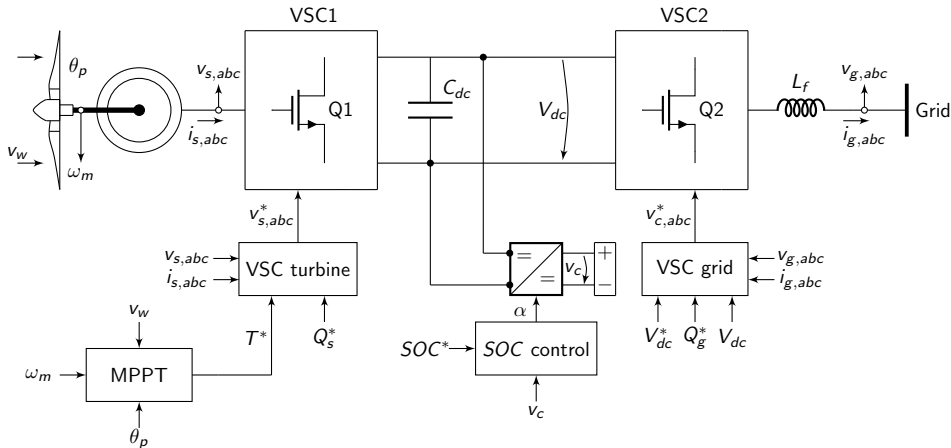


Figure 5: Scheme of the full system with the turbine, the converters, and the energy storage unit

The machine-side converter has to be controlled so as to extract the maximum power from the wind.

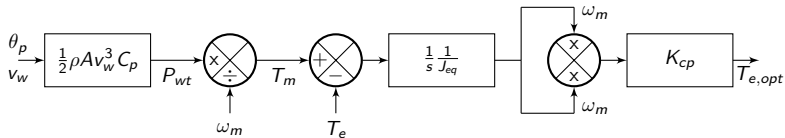


Figure 6: Block diagram of the MPPT

The key part is the quadratic relationship between speed and torque:

$$K_{cp} = \frac{1}{2} \rho A \left(\frac{D}{2} \right)^3 \left(\frac{c_1}{c_2^2 c_7^4} (c_2 + c_6 c_7)^3 e^{-(c_2 + c_6 c_7)/c_2} \right). \quad (2)$$

Two references are received: reactive power and optimal torque.

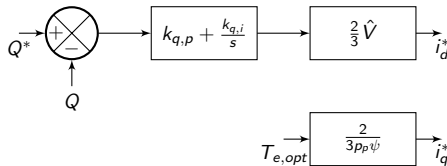


Figure 7: Reactive power control and current references calculation

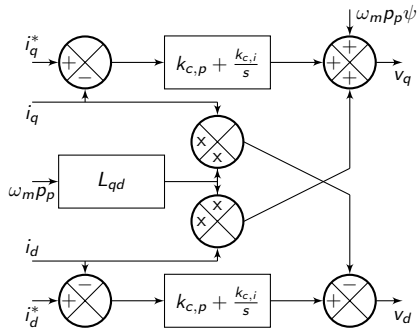


Figure 8: Inner current control loop

With the inner current control loop, the current references are transformed into the qd voltages to synthesize.

Two references are received: the DC bus voltage and the reactive power to exchange with the grid.

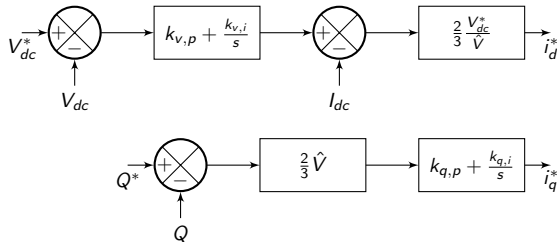


Figure 9: Reactive power control and DC voltage control loop

Just like before, an inner current control loop is also present.

Responsible for controlling the charge and discharge processes of the supercapacitor.

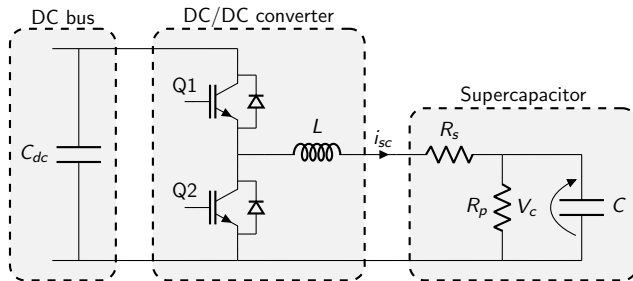


Figure 10: DC/DC buck converter with the supercapacitor

Switches $Q1$ and $Q2$ are turned on and off according to the desired duty cycle D .

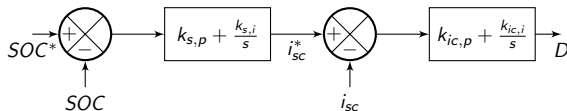


Figure 11: Control diagram of the SOC of the supercapacitor

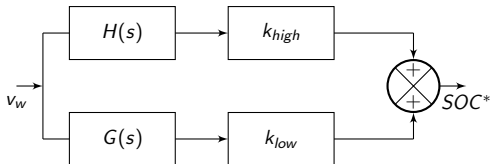


Figure 12: Calculation of the reference of the SOC

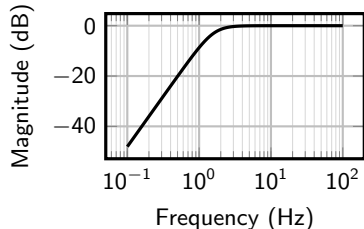
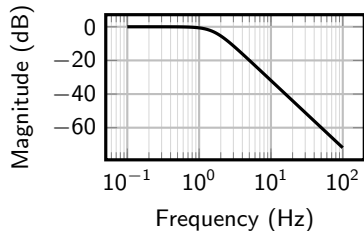


Figure 13: Bode plot of $H(s)$ and $G(s)$

The supercapacitor is sized based on a sinusoidal perturbation:

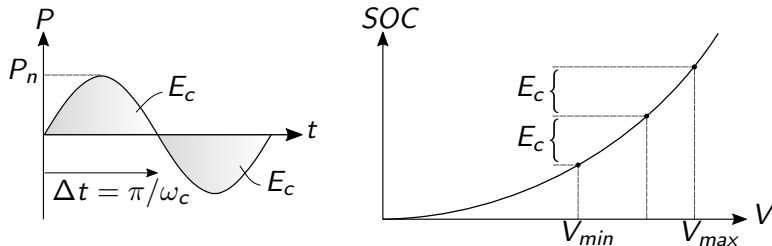


Figure 14: Perturbation and SOC as a function of the voltage of the supercapacitor

$$C = \frac{8 \frac{P_n}{\omega_c}}{V_{max}^2 - V_{min}^2}. \quad (3)$$

- ▶ For the considered case study, $C = 0.91 \text{ F}$.
- ▶ Configuration of 4 parallel branches and about 1600 series cells.
- ▶ In total, they occupy about 0.382 m^3 and last for 500000 cycles.

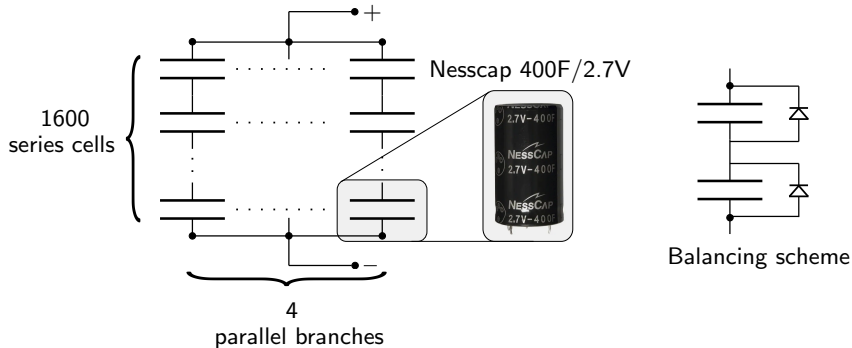


Figure 15: Chosen configuration of cells

Apart from qualitative observations, quantitative indicators are considered.
Assessment based on:

- ▶ Maximum variation in the output power:

$$\Delta P = \max(P) - \min(P). \quad (4)$$

- ▶ Roughness index:

$$RI = \sum_{i=1}^{n-1} [P(i+1) - P(i)]^2. \quad (5)$$

- ▶ Simple moving average:

$$SMA_k = \frac{1}{k} \sum_{i=n-k-1}^n P(i). \quad (6)$$

Example in a two-bus system

Smart grids: from traditional to modernized resilient systems

Group 2

Introduction

Phase 1

Results

Problems identification

Context

Aim of the project

Models

General scheme

MPPT

Machine-side converter

Grid-side converter

Supercapacitor control

Sizing

Calculations

Configuration

Results

Indicators

Example

Conclusions

19 / 23

The supercapacitor mitigates the fluctuations to obtain a smoother power profile.

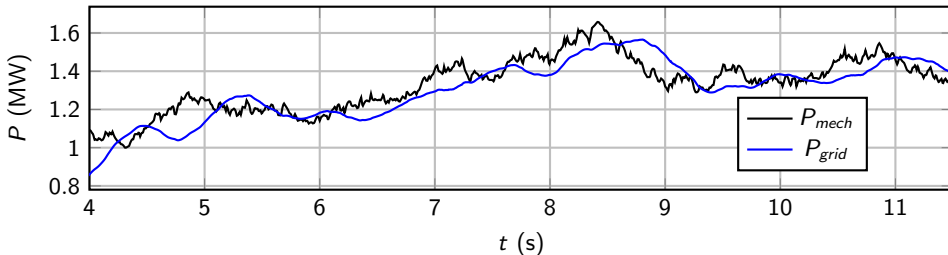


Figure 16: Mechanical power and active power exchanged with the grid

Indicator	P_{mech}	P_{grid}
ΔP (MW)	0.531	0.439
RI (MW ²)	0.066	0.003

Table 3: Numerical indicators results

Smart grids: from traditional to modernized resilient systems

Group 2

Introduction

Phase 1

Results

Problems identification

Context

Aim of the project

Models

General scheme

MPPT

Machine-side converter

Grid-side converter

Supercapacitor control

Sizing

Calculations

Configuration

Results

Indicators

Example

Conclusions

20 / 23

- ▶ The combination of type-IV wind turbines with an energy storage device offers great controllability.
- ▶ The supercapacitor manages to reduce the fluctuations in power.
- ▶ It was preferable to prioritize the low frequencies. However, other control strategies may be equally convenient, if not more.

Smart grids: from traditional to modernized resilient systems

Group 2

Introduction

Phase 1

Results

Problems identification

Context

Aim of the project

Models

General scheme

MPPT

Machine-side converter

Grid-side converter

Supercapacitor control

Sizing

Calculations

Configuration

Results

Indicators

Example

Conclusions

21 / 23

Bibliography

1. F. Blaabjerg, F. Iov, R. Teodorescu, and Z. Chen, "Power electronics in renewable energy systems," in 2006 12th International Power Electronics and Motion Control Conference, IEEE, 2006, pp. 1–17.
2. H. Abu-Rub, M. Malinowski, and K. Al-Haddad, Power electronics for renewable energy systems, transportation and industrial applications. John Wiley & Sons, 2014.
3. M.-H. Ryu, H.-S. Kim, J.-W. Baek, H.-G. Kim, and J.-H. Jung, "Effective test bed of 380-v dc distribution system using isolated power converters," IEEE transactions on industrial electronics, vol. 62, no. 7, pp. 4525–4536, 2015.
4. IRENA, "Renewable capacity statistics 2021," Abu Dabi, United Emirate States, Annual report, 2021.
5. F. Blaabjerg, M. Liserre, and K. Ma, "Power electronics converters for wind turbine systems," IEEE Transactions on industry applications, vol. 48, no. 2, pp. 708–719, 2011.
6. O. Tremblay, R. Gagnon, and M. Fecteau, "Real-time simulation of a fully detailed type-iv wind turbine," submitted to IPST, vol. 13, pp. 18–20, 2013.
7. N. Espinoza, M. Bongiorno, and O. Carlson, "Frequency characterization of type-iv wind turbine systems," in 2016 IEEE Energy Conversion Congress and Exposition (ECCE), IEEE, 2016, pp. 1–8.
8. G. He, Q. Chen, C. Kang, Q. Xia, and K. Poola, "Cooperation of wind power and battery storage to provide frequency regulation in power markets," IEEE Transactions on Power Systems, vol. 32, no. 5, pp. 3559–3568, 2016.
9. G. Mandic, A. Nasiri, E. Ghotbi, and E. Muljadi, "Lithium-ion capacitor energy storage integrated with variable speed wind turbines for power smoothing," IEEE Journal of emerging and selected topics in power electronics, vol. 1, no. 4, pp. 287–295, 2013.
10. W. C. de Carvalho, R. P. Bataglioli, R. A. Fernandes, and D. V. Coury, "Fuzzy-based approach for power smoothing of a full-converter wind turbine generator using a supercapacitor energy storage," Electric Power Systems Research, vol. 184, p. 106 287, 2020.
11. P. Garasi, M. Watanabe, and Y. Mitani, "Power smoothing of wind turbine generator using fuzzy-pi pitch angle controller," in 2014 Australasian Universities Power Engineering Conference (AUPEC), IEEE, 2014, pp. 1–5.
12. O. P. Mahela and A. G. Shaik, "Comprehensive overview of grid interfaced wind energy generation systems," Renewable and Sustainable Energy Reviews, vol. 57, pp. 260–281, 2016.
13. G. O. Suvire, M. G. Molina, and P. E. Mercado, "Improving the integration of wind power generation into ac microgrids using flywheel energy storage," IEEE Transactions on smart grid, vol. 3, no. 4, pp. 1945–1954, 2012.
14. L. Qu and W. Qiao, "Constant power control of dfig wind turbines with supercapacitor energy storage," IEEE Transactions on Industry Applications, vol. 47, no. 1, pp. 359–367, 2010.
15. A. K. Arani, H. Karami, G. Gharehpetian, and M. Hejazi, "Review of flywheel energy storage systems structures and applications in power systems and microgrids," Renewable and Sustainable Energy Reviews, vol. 69, pp. 9–18, 2017.
16. C. Abbey and G. Joos, "Supercapacitor energy storage for wind energy applications," IEEE transactions on Industry applications, vol. 43, no. 3, pp. 769–776, 2007.
17. M. Ammar and G. Joós, "A short-term energy storage system for voltage quality improvement in distributed wind power," IEEE Transactions on Energy Conversion, vol. 29, no. 4, pp. 997–1007, 2014.

Smart grids: from traditional to modernized resilient systems

Group 2

Introduction

Phase 1

Results

Problems identification

Context

Aim of the project

Models

General scheme

MPPT

Machine-side converter

Grid-side converter

Supercapacitor control

Sizing

Calculations

Configuration

Results

Indicators

Example

Conclusions

18. J. P. Queralt and O. G. Bellmunt, "Control of voltage source converters for distributed generation in microgrids," PhD thesis, Universitat Politècnica de Catalunya, 2015.

19. M. Raza and O. Gomis-Bellmunt, "Control system of voltage source converter to interconnect offshore ac hub with multiple on-shore grids," in 2015 International Conference on Renewable Energy Research and Applications (ICRERA), IEEE, 2015, pp. 677–682.

20. M. Ragheb, "Wind energy conversion theory, betz equation," Wind Energie, 2014.

21. T. Ackermann, Wind power in power systems. John Wiley & Sons, 2012.

22. F. Diaz-González, A. Sumper, O. Gomis-Bellmunt, and F. D. Bianchi, "Energy management of flywheel-based energy storage device for wind power smoothing," Applied energy, vol. 110, pp. 207–219, 2013.

23. A. Junyent-Ferré, O. Gomis-Bellmunt, A. Sumper, M. Sala, and M. Mata, "Modeling and control of the doubly fed induction generator wind turbine," Simulation Modelling Practice and Theory, vol. 18, no. 9, pp. 1365–1381, 2010.

24. T.-t. Liu, Y. Tan, G. Wu, and S.-m. Wang, "Simulation of pmsm vector control system based on matlab/simulink," in 2009 international conference on measuring technology and mechatronics automation, IEEE, vol. 2, 2009, pp. 343–346.

25. H. Mahmood, D. Michaelson, and J. Jiang, "Reactive power sharing in islanded microgrids using adaptive voltage droop control," IEEE Transactions on Smart Grid, vol. 6, no. 6, pp. 3052–3060, 2015.

Smart grids: from traditional to modernized resilient systems

Víctor Escala García
Josep Fanals Batllori
Pol Heredia Julbe
Roger Izquierdo Toro
Palina Nicolas

Smart Grids

January 13, 2021